Current Journal of Applied Science and Technology

40(1): 10-31, 2021; Article no.CJAST.62974
ISSN: 2457-1024
(Past name: British Journal of Applied Science & Technology, Past ISSN: 2231-0843, NLM ID: 101664541)

Unveiling Perturbing Effects of P-R Drag on Motion around Triangular Lagrangian Points of the Photogravitational Restricted Problem of Three Oblate Bodies

Tajudeen Oluwafemi Amuda[1*], Oni Leke[2] and Abdulrazaq Abdulraheem[3]

[1]Department of Mathematics, Faculty of Sciences, Air Force Institute of Technology, Kaduna, Kaduna State, Nigeria.
[2]Department of Mathematics, Statistics and Computer Science, College of Science, University of Agriculture, P.M.B. 2373, North-Bank, Makurdi, Nigeria.
[3]Department of Statistics and Mathematical Sciences, Kwara State University, Malete-Ilorin Nigeria.

Authors' contributions

This work was carried out in collaboration among all authors. All authors read and approved the final manuscript.

Article Information

DOI: 10.9734/CJAST/2021/v40i131201
Editor(s):
(1) Dr. Vyacheslav O. Vakhnenko, Subbotin Institute of Geophysics, National Academy of Sciences of Ukrainian, Ukraine.
Reviewers:
(1) Eshetu Dadi Gurmu, Wollega University, Ethiopia.
(2) Youssef EL Foutayeni, Hassan II University of Casablanca, Morocco.
Complete Peer review History: http://www.sdiarticle4.com/review-history/62974

Original Research Article

Received 10 September 2020
Accepted 16 November 2020
Published 15 January 2021

ABSTRACT

The perturbing effects of the Poynting-Robertson drag on motion of an infinitesimal mass around triangular Lagrangian points of the circular restricted three-body problem under small perturbations in the Coriolis and centrifugal forces when the three bodies are oblate spheroids and the primaries are emitters of radiation pressure, is the focus of this paper. The equations governing the dynamical system have been derived and locations of triangular Lagrangian points are determined. It is seen that the locations are influenced by the perturbing forces of centrifugal perturbation and the oblateness, radiation pressure and, P-R drag of the primaries. Using the software *Mathematica,* numerical analysis are carried out to demonstrate how the dynamical elements: mass ratio, oblateness, radiation pressure, P-R drag and centrifugal perturbation influence the positions of

**Corresponding author: E-mail: teejaymath@gmail.com;*

triangular equilibrium points, zero velocity surfaces and the stability. Our investigation reveals that, though the radiation pressure, oblateness and centrifugal perturbation decrease region of stability when motion is stable, however, they are not the influential forces of instability but the P-R drag. In the region when motion around the triangular points are stable an inclusion of the P-R drag of the bigger primary even by an almost negligible value of $1.04548*10^{-9}$ overrides other effect and changes stability to instability. Hence, we conclude that the P-R drag is a strong perturbing force which changes stability to instability and motion around triangular Lagrangian points remain unstable in the presence of the P-R drag.

Keywords: Restricted three-body problem; triangular lagrangian points; radiation pressure; oblateness; P-R drag.

1. INTRODUCTION

The restricted three-body problem (R3BP) constitutes one of the most important problems in dynamical astronomy. The study of this problem is of great theoretical, practical and educational relevance. The investigation of this problem in its several versions has been the focus of continuous and intense research activity for centuries The R3BP is a modify model of the three-body problem [1] which illustrate motion of an infinitesimal mass under gravitational attraction of two bodies called primaries. This problem under different formulations has had important implications in some scientific fields such as, galactic dynamics, chaos theory, molecular physics and celestial mechanics, among others.

The classical problem of Szebehely [2] did not consider the primaries as sources of radiation pressure or as non-spherical bodies. In view of this, several studies when one or both primaries have radiation pressure and are oblate spheroids have been formulated and examined. Notable among these are Sharma and Subba Rao [3], Singh and Ishwar [4], Khanna and Bhatnagar [5], Abdul Raheem and Singh [6], Singh and Leke [7,8,9], Singh and Haruna [10], Singh and Amuda [11]. Another characterization of the primaries which has to do with radiation force is the perturbing effect of Poynting–Robertson (P–R) drag. This force is a component of the radiation force and sweep small particles of the solar system into the Sun at a cosmically rapid rate, thereby justifying its inclusion in the modify model of the R3BP by authors such as Schuerman [12], Murray [13], Ragos and Zafiropoulos [14], Kushvah [15], Das et al. [16], and recently Singh and Amuda [17].

Finally, in the classical R3BP the infinitesimal mass is assumed to move only under the mutual gravitational force of the primaries, but in practice, Coriolis and centrifugal forces are effective and small perturbations affect these forces. Examples include; small deviation of disc stars in circular orbits and motion of a close artificial satellite of the Earth perturbed by the atmospheric friction and the oblateness of the Earth. Studies of this type of problem include, Bhatnagar and Hallan [18], Abdul Raheem and Singh [6], Singh et al. [7,8], among other. Singh and Leke [19] studied the periodic motion and stability of spherical dust grain particle around triangular Lagrangian points, in the neighborhood of a post-AGB binary, enclosed by circumbinary disc under the effect of the Coriolis and centrifugal perturbations. Singh and Haruna [20] examined motion of an oblate-shaped infinitesimal mass under effects of small perturbations in the Coriolis and centrifugal forces when the primaries are radiating oblate spheroid. Hence, it is reasonable in this study, to consider when Coriolis and centrifugal forces are slightly perturbed.

In this paper, we aim to locate and examine the stability of triangular Lagrangian points of the restricted problem of three bodies under the combined effect of oblateness, perturbations, radiation and P-R drag. This study extends earlier work of Singh and Haruna [10] by including the P-R drag into the radiation forces of both primaries. The equations of motion, locations of the triangular Lagrangian points and their linear stability are discussed. The zero velocity curves have also been examined under the combined actions of the perturbing forces. The paper is organized as follows: Section 2 describes the equations of motion of the model while section 3 focuses on the position of the triangular points. The zero velocity surfaces and stability of the triangular Lagrangian points are discussed in section 4 and 5, respectively while section 6discuss and concludes the paper.

2. THE MODEL EQUATIONS

The equations of motion of an oblate-shaped infinitesimal mass in the gravitational forces of two radiating oblate spheroidal primaries under effects of small perturbations in the Coriolis and centrifugal forces have the following form Singh and Haruna [10]:

$$\ddot{x}-2\alpha n\dot{y}=n^2\beta x-\frac{(1-\mu)(x+\mu)q_1}{r_1^3}-\frac{3(1-\mu)A_1(x+\mu)q_1}{2r_1^5}-\frac{\mu q_2(x+\mu-1)}{r_2^3}-\frac{3\mu(x+\mu-1)A_2q_2}{2r_2^5}$$
$$-\frac{3(1-\mu)(x+\mu)A_3}{2r_1^5}-\frac{3\mu(x+\mu-1)A_3}{2r_2^5}$$
$$\ddot{y}+2\alpha n\dot{x}=n^2\beta y-\frac{(1-\mu)yq_1}{r_1^3}-\frac{3(1-\mu)yA_1q_1}{2r_1^5}-\frac{\mu q_2y}{r_2^3}-\frac{3\mu yA_2q_2}{2r_2^5}-\frac{3(1-\mu)A_3y}{2r_1^5}$$
$$-\frac{3\mu yA_3}{2r_2^5} \tag{1}$$

Where

$$r_1^2=(x+\mu)^2+y^2,\ r_2^2=(x+\mu-1)^2+y^2, \tag{2}$$

$$n^2=1+\frac{3}{2}A_1+\frac{3}{2}A_2, \tag{3}$$

The distances between the infinitesimal mass from the primaries are r_1 and r_2, respectively, while $A_i(i=1,2,3)$ are the oblateness coefficients of the bigger primary, smaller primary and the infinitesimal mass, respectively and n is the mean motion defined by the oblateness of the primaries. μ is the mass parameter of the configuration and is expressed as the ratio of the mass of the smaller primary to the sum of the masses of the both primaries and is such that $0<\mu\leq\frac{1}{2}$. The radiation pressure factors of the bigger and smaller primaries are represented by $q_i(i=1,2)$, respectively while the parameters α and β are the small perturbations in the Coriolis and centrifugal forces, respectively and are such that $\alpha=1+\varepsilon$, $\beta=1+\varepsilon' : |\varepsilon|<<1\ \ |\varepsilon'|<<1$

The formulation by Singh and Haruna [10] given in equations (1) took into account the radiation force owning to the gravitational force and radiation pressure. They did not consider the other component of the radiation force: (i) forces arising from the Doppler shift and, (ii) the absorption and subsequent re-emission of the incident radiation. These forces are what make up what is referred to, as the Poynting-Robertson (P-R) drag Schuerman [12].

Hence, we include P-R drag and follow the methodology in Singh and Amuda (2017) to get the modified equations of motion:

$$\ddot{x}-2n\alpha\dot{y}=U_x,\qquad \ddot{y}+2n\alpha\dot{x}=U_y, \tag{4}$$

Where

$$U_x = n^2\beta x - \frac{(1-\mu)(x+\mu)\,q_1}{r_1^3} - \frac{3(1-\mu)A_1(x+\mu)\,q_1}{2r_1^5} - \frac{\mu q_2(x+\mu-1)}{r_2^3} - \frac{3\mu(x+\mu-1)\,A_2\,q_2}{2r_2^5}$$
$$-\frac{3(1-\mu)A_3(x+\mu)}{2r_1^5} - \frac{3\mu(x+\mu-1)\,A_3}{2r_2^5} - \frac{W_1}{r_1^2}\left[\frac{(x+\mu)}{r_1^2}\{(x+\mu)\dot{x} + y\dot{y} + z\dot{z}\} + \dot{x} - ny\right]$$
$$-\frac{W_2}{r_2^2}\left[\frac{(x+\mu-1)}{r_2^2}\{(x+\mu-1)\dot{x} + y\dot{y} + z\dot{z}\} + \dot{x} - ny\right],$$
$$U_y = n^2\beta y - \frac{(1-\mu)y\,q_1}{r_1^3} - \frac{3(1-\mu)y\,A_1 q_1}{2r_1^5} - \frac{\mu q_2\,y}{r_2^3} - \frac{3\mu y\,A_2\,q_2}{2r_2^5} - \frac{3(1-\mu)A_3\,y}{2r_1^5} - \frac{3\mu y A_3}{2r_2^5}$$
$$-\frac{W_1}{r_1^2}\left[\frac{y}{r_1^2}\{(x+\mu)\dot{x} + y\dot{y} + z\dot{z}\} + \dot{y} + n(x+\mu)\right] - \frac{W_2}{r_2^2}\left[\frac{y}{r_2^2}\{(x+\mu-1)\dot{x} + y\dot{y} + z\dot{z}\} + \dot{y} + n(x+\mu-1)\right],$$

$$W_1 = \frac{(1-\mu)(1-q_1)}{c_d},\ W_2 = \frac{\mu(1-q_2)}{c_d}.$$

$W_i(i=1{,}2)$ are the P-R drag of the bigger and smaller primaries, respectively; and c_d is the dimensionless velocity of light.

These equations of motion of the setup are affected by the combined effects of oblateness of the three bodies, small perturbations in the Coriolis and centrifugal forces, radiation pressure and P-R drag, of the primaries. Next, we discuss the locations of triangular Lagrangian points of the infinitesimal mass.

3. LOCATIONS OF TRIANGULAR LAGRANGIAN POINTS

The Lagrangian points or equilibrium points of the R3BP are widely used in many branches of astronomy, both for constant and variable masses (e.g., in the Roche model for binary star systems); Luk'yanov [21]. Another importance of these points in astronomy is that they indentify locations where particles either can be held (L_4 and L_5) or will move through with a minimum expenditure of energy. In the theory of binary star evolution, the more massive component will expand as it ages until material meets one of the Lagrangian points Collins [22]. To get the locations of triangular Lagrangian points of our problem, we solve equations (4) when $U_x = 0, U_y = 0$, $\dot{x} = \dot{y} = \ddot{x} = \ddot{y} = 0$ and $y \neq 0$ such that

$$n^2\beta x - \frac{(1-\mu)(x+\mu)\,q_1}{r_1^3} - \frac{3(1-\mu)A_1(x+\mu)\,q_1}{2r_1^5} - \frac{3(1-\mu)A_3(x+\mu)}{2r_1^5} - \frac{\mu q_2(x+\mu-1)}{r_2^3}$$
$$-\frac{3\mu(x+\mu-1)\,A_2\,q_2}{2r_2^5} - \frac{3\mu(x+\mu-1)\,A_3}{2r_2^5} + \frac{W_1 n\,y}{r_1^2} + \frac{W_2 n\,y}{r_2^2} = 0, \tag{5}$$

and,

$$\left[n^2\beta - \frac{(1-\mu)q_1}{r_1^3} - \frac{3(1-\mu)q_1A_1}{2r_1^5} - \frac{3(1-\mu)A_3}{2r_1^5} - \frac{\mu q_2}{r_2^3} - \frac{3\mu A_2 q_2}{2r_2^5} - \frac{3\mu A_3}{2r_2^5}\right]y$$
$$-\frac{W_1 n(x+\mu)}{r_1^2} - \frac{W_2 n(x+\mu-1)}{r_2^2} = 0. \tag{6}$$

Equations (5) and (6) contain nine (9) parameters, therefore to solve these equations for x and y, we shall use the small perturbation method. Observe that when the P-R drag and oblateness of the bodies are ignored, equations (5) and (6) reduce to

$$x\left[\beta - \frac{(1-\mu)q_1}{r_1^3} - \frac{\mu q_2}{r_2^3}\right] - (1-\mu)\mu\left[\frac{q_1}{r_1^3} - \frac{q_2}{r_2^3}\right] = 0$$

And

$$\beta - \frac{(1-\mu)q_1}{r_1^3} - \frac{\mu q_2}{r_2^3} = 0.$$

Now, $\mu(1-\mu)$ does not vanish and so solving the above pair of equation, we get

$$r_1 = \left(\frac{q_1}{\beta}\right)^{\frac{1}{3}}, \; r_2 = \left(\frac{q_2}{\beta}\right)^{\frac{1}{3}}. \tag{7}$$

Therefore with the help of equation (7), the solutions of equations (5) and (6), are

$$r_1 = \left(\frac{q_1}{\beta}\right)^{\frac{1}{3}} + \varepsilon_1, \; r_2 = \left(\frac{q_2}{\beta}\right)^{\frac{1}{3}} + \varepsilon_2; \qquad |\varepsilon_i| << 1 \; (i = 1,2) \tag{8}$$

To get the exact x-coordinate of the triangular point, we subtract the second equation of (2) from the first, to get

$$x = \frac{1}{2} - \mu + \frac{r_1^2 - r_2^2}{2} \tag{9}$$

Substituting equations (8) in (9), we get

$$x = x_0 + \left(\frac{q_1}{\beta}\right)^{\frac{1}{3}}\varepsilon_1 - \left(\frac{q_2}{\beta}\right)^{\frac{1}{3}}\varepsilon_2 \tag{10}$$

where

$$x_0 = \frac{1}{2} - \mu + \frac{q_1^{\frac{2}{3}} - q_2^{\frac{2}{3}}}{2\beta^{\frac{2}{3}}} \tag{11}$$

Now from the first equation of (2), we get

$$y = \pm y_0 \left[1 + \frac{1}{2y_0^2 \beta^{\frac{1}{3}}} \left(q_1^{\frac{1}{3}} \varepsilon_1 + q_2^{\frac{1}{3}} \varepsilon_2 \right) - \frac{1}{2y_0^2 \beta} \left(q_1^{\frac{2}{3}} - q_2^{\frac{2}{3}} \right) \left(q_1^{\frac{1}{3}} \varepsilon_1 - q_2^{\frac{1}{3}} \varepsilon_2 \right) \right] \tag{12}$$

where

$$y_0 = \pm \frac{1}{2} \left[-1 + \frac{1}{2\beta^{\frac{2}{3}}} \left(q_1^{\frac{1}{3}} + q_2^{\frac{1}{3}} \right) + \frac{1}{2\beta^{\frac{4}{3}}} \left(q_1^{\frac{2}{3}} - q_2^{\frac{2}{3}} \right)^2 \right]^{\frac{1}{2}} \tag{13}$$

Looking at equations (10) and (12) the perturbing forces owing to the oblateness and P-R drag are not visible because they are embedded in ε_i. Therefore, to determine ε_i, we first substitute equations (3), (8), (10) and (12) into equations (5) and (6), respectively; we simplify by neglecting higher order terms of small quantities, to get the respective equations:

$$a_1 \varepsilon_1 + b_1 \varepsilon_2 = c_1 \tag{14}$$
$$a_2 \varepsilon_1 + b_2 \varepsilon_2 = c_2 \tag{15}$$

Where

$$a_1 = 3(1-\mu)(x_0 + \mu)\beta^{\frac{4}{3}} q_1^{-\frac{1}{3}}, \qquad b_1 = 3\mu(x_0 + \mu - 1)\beta^{\frac{4}{3}} q_2^{-\frac{1}{3}}$$

$$c_1 = \frac{3}{2}\beta^{\frac{5}{3}} \Big[-x_0 \beta^{-\frac{2}{3}} (A_1 + A_2) + x_0(1-\mu) q_1^{-\frac{2}{3}} A_1 + \mu x_0 q_2^{-\frac{2}{3}} A_2 - (1-\mu) x_0 q_1^{-\frac{5}{3}} A_3 + \mu x_0 q_2^{-\frac{5}{3}} A_3$$
$$+ (1-\mu) q_1^{-\frac{2}{3}} A_1 - (1-\mu) q_2^{-\frac{2}{3}} A_2 + (1-\mu) q_1^{-\frac{5}{3}} A_3 - (1-\mu) q_2^{-\frac{5}{3}} A_3 - \frac{2y_0}{3\beta} q_1^{-\frac{2}{3}} (W_1 + W_2) \Big]$$

$$a_2 = 3(1-\mu) y_0 \beta^{\frac{4}{3}} q_1^{-\frac{1}{3}}, \quad b_2 = 3\mu y_0 \beta^{\frac{4}{3}} q_2^{-\frac{1}{3}}$$

$$c_2 = \frac{3\beta^{\frac{5}{3}}}{2} \Big[-\beta^{-\frac{2}{3}} (A_1 + A_2) y_0 + (1-\mu) y_0 q_1^{\frac{-2}{3}} A_1 + \mu y_0 q_2^{-\frac{2}{3}} A_2 + (1-\mu) y_0 q_1^{-\frac{5}{3}} A_3 + \mu y_0 q_2^{-\frac{5}{3}} A_3$$
$$+ \frac{2}{3}(x_0 + \mu) q_1^{-\frac{2}{3}} \beta^{-\frac{4}{3}} W_1 + \frac{2}{3}(x_0 + \mu - 1) q_2^{-\frac{2}{3}} \beta^{-\frac{4}{3}} W_2 \Big]$$

Equations (14) and (15) is a system of two equations in two variables ε_1 and ε_2. These variables can be determined using the Cramer's Rule given by

$$\varepsilon_1 = \frac{b_2 c_1 - b_1 c_2}{a_1 b_2 - a_2 b_1}, \quad \varepsilon_2 = \frac{a_1 c_2 - a_2 c_1}{a_1 b_2 - a_2 b_1}$$

Substituting the coefficients $a_i, b_i, c_i \ (i = 1,2)$, and applying equations (11) and (13), we get

$$\varepsilon_1 = -\frac{1}{3}\left[\frac{3}{2}(A_2 - A_3) + \left(\frac{1}{\sqrt{3}(1-\mu)}\right)W_1 + \left(\frac{2}{\sqrt{3}(1-\mu)}\right)W_2\right]$$

$$\varepsilon_2 = -\frac{1}{3}\left[\frac{3}{2}(A_1 - A_3) - \left(\frac{2}{\mu\sqrt{3}}\right)W_1 - \left(\frac{1}{\mu\sqrt{3}}\right)W_2\right] \tag{16}$$

Finally, substituting equations (16) in equations (10) and (12), we get the locations of the triangular Lagrangian points:

$$x = \frac{1}{2} - \mu - \frac{1}{\beta^{2/3}}\left[\frac{1}{3}(1-q_1) + \frac{1}{3}(1-q_2) + \frac{1}{2}(A_1 - A_2)\beta^{2/3} - \frac{\sqrt{3}(2-\mu)W_1}{9\mu(1-\mu)} - \frac{\sqrt{3}(1+\mu)W_2}{9\mu(1-\mu)}\right]$$

and (17)

$$y = \pm\frac{\sqrt{4-\beta^{2/3}}}{2\beta^{1/3}}\left[1 - \frac{2}{4-\beta^{2/3}}\left\{\frac{4-\beta^{2/3}}{9.\mu(1-\mu)}\left(\frac{3}{2}\mu W_1 + \frac{3}{2}\mu W_2 - W_1 - \frac{1}{2}W_2\right) + \frac{1}{3}(1-q_1) + \frac{1}{3}(1-q_2) + (A_1 + A_2) - \frac{1}{2}(A_1 + A_2 + 2A_3)\beta^{2/3}\right\}\right]$$

The solutions are defined by the radiation pressure and P-R drag of the primaries, the centrifugal force perturbation and oblateness of the three bodies, and the points are denoted by $L_{4,5}(x, \pm y)$.

To do our numerical exploration, we consider the binary system **Kruger 60**having masses $0.271M_0$ and $0.176M_0$ with luminosity 0.01 and 0.0034, respectively. This system has a binary separation of 9.5 AU and the radiation pressure is taken as 0.99992 and 0.99996, respectively. This is shown in Table 1 below

Table 1. Numerical data for Kruger 60

Binary	Luminosity (L_0) L_1 L_2	Mass (M_0) M_1 M_2	Radiation pressure (q_i) q_1	q_2	Binary distance (AU) a	Velocity of light c_d
Kruger 60	0.01 0.0034	0.271 0.176	0.99992	0.99996	9.5	46393.84

Using the software *Mathematica* [23], we compute numerically in Tables 2-5 the positions of triangular equilibrium points given by equation (17) with the data presented in Table 1. The three-dimensional plots of the triangular Lagrangian points under the perturbing effects of the mass parameter, oblateness, radiation, small perturbation in the centrifugal force and the P-R drag are presented in Figs. 1-5.

Table 2. Effect of oblateness A_1 on $L_{4,5}$

ε'	q_1	q_2	A_1	A_2	A_3	W_1	W_2	x_4	$\pm y_4$
0.001	0.99992	0.99996	0	0.2	0.1	0	0	0.0062867	0.865617
,,	,,	,,	0.01	"	"	$1.04548*10^{-9}$	$3.39442*10^{-10}$	0.0112867	0.862731
,,	,,	,,	0.05	"	"	,,	,,	0.0312867	0.851184
,,	,,	,,	0.1	"	"	,,	,,	0.0562867	0.836750
,,	,,	,,	0.15	"	"	,,	,,	0.0812867	0.822316
,,	,,	,,	0.2	"	"	,,	,,	0.1062870	0.807882

Table 3. Effect of oblateness A_2 on $L_{4,5}$

ε'	q_1	q_2	A_1	A_2	A_3	W_1	W_2	x_4	$\pm y_4$
0.001	0.99992	0.99996	0.15	0	0.1	0	0	0.181287	0.880051
,,	,,	,,	"	0.01	"	$1.04548*10^{-9}$	$3.39442*10^{-10}$	0.176287	0.877164
,,	,,	,,	"	0.05	"	,,	,,	0.156287	0.865617
,,	,,	,,	"	0.1	"	,,	,,	0.131287	0.851184
,,	,,	,,	"	0.15	"	,,	,,	0.106287	0.836750
,,	,,	,,	"	0.2	"	,,	,,	0.081287	0.822316

Table 4. Effect of oblateness A_3 on $L_{4,5}$

ε'	q_1	q_2	A_1	A_2	A_3	W_1	W_2	x_4	$\pm y_4$
0.001	0.99992	0.99996	0.15	0.2	0	0	0	0.0812867	0.764581
,,	0.99992	0.99996	"	"	0.01	$1.04548*10^{-9}$	$3.39442*10^{-10}$	0.0812867	0.770355
,,	,,	,,	"	"	0.05	,,	,,	0.0812867	0.793449
,,	,,	,,	"	"	0.1	,,	,,	0.0812867	0.822316
,,	,,	,,	"	"	0.15	,,	,,	0.0812867	0.851184
,,	,,	,,	"	"	0.2	,,	,,	0.0812867	0.880051

Table 5. Effect of small perturbation ε' in the centrifugal force on $L_{4,5}$

ε'	q_1	q_2	A_1	A_2	A_3	W_1	W_2	x_4	$\pm y_4$
0	0.99992	0.99996	0.15	0.2	0.1	0	0	0.0812867	0.822701
0.0001	0.99992	0.99996	"	"	"	$1.04548*10^{-9}$	$3.39442*10^{-10}$	0.0812867	0.822663
0.001	"	"	"	"	"	"	"	0.0812867	0.822316
0.01	"	"	"	"	"	"	"	0.0812867	0.818852
0.05	"	"	"	"	"	"	"	0.0812867	0.803456
0.1	"	"	"	"	"	"	"	0.0812867	0.784211

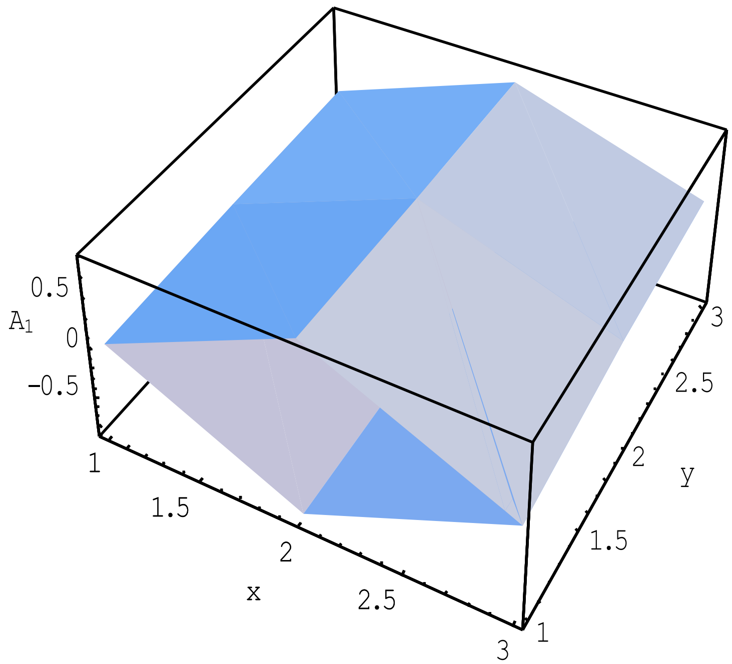

Fig. 1. 3D plots of $L_{4,5}$ **as a function of** A_1 **when** $q_1 = 0.99992$, $q_2 = 0.99996$, $A_2 = 0.2$, $A_3 = 0.1$, **and** $\varepsilon' = 0.001$

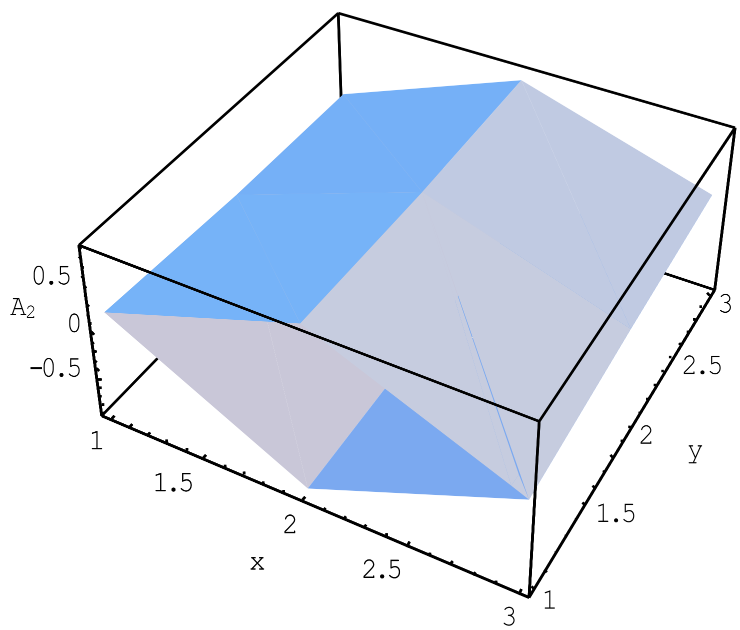

Fig. 2. 3D plots of $L_{4,5}$ **as a function of** A_2 **when** $q_1 = 0.99992$, $q_2 = 0.99996$, $A_1 = 0.15$, $A_3 = 0.1$, **and** $\varepsilon' = 0.001$

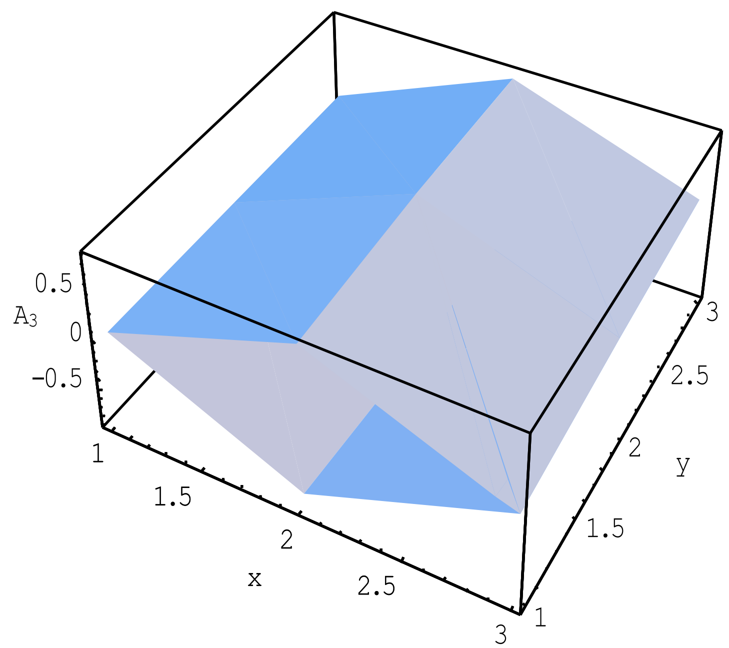

Fig. 3. 3D plots of $L_{4,5}$ **as a function of** A_3 **when** $q_1 = 0.99992$, $q_2 = 0.99996$, $A_1 = 0.15$, $A_2 = 0.2$, **and** $\varepsilon' = 0.001$

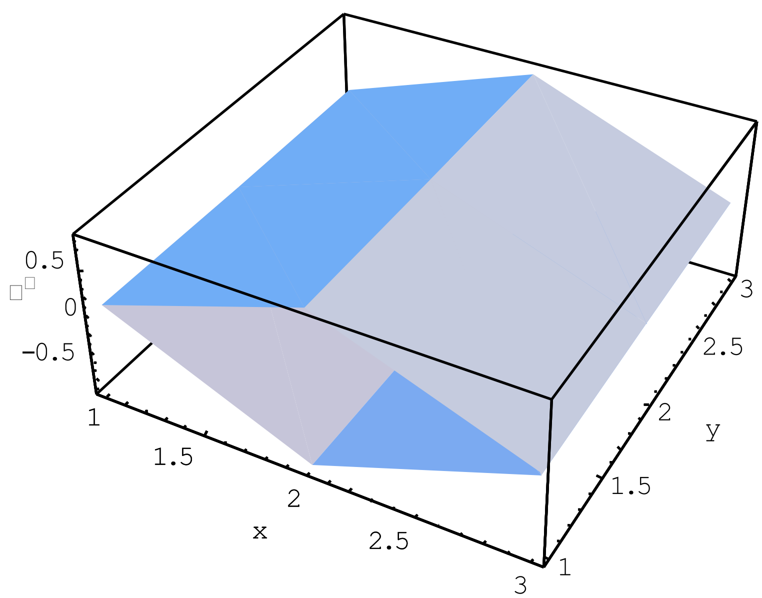

Fig. 4. 3D plots of $L_{4,5}$ **as a function of** ε' **when** $q_1 = 0.99992$, $q_2 = 0.99996$, $A_1 = 0.15$, $A_2 = 0.2$, **and** $A_3 = 0.1$

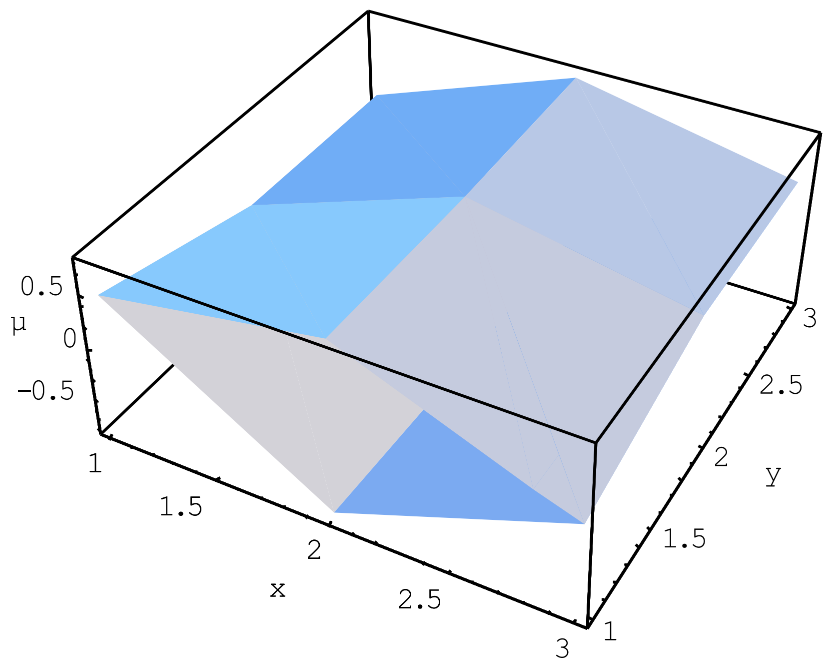

Fig. 5. 3D plots of $L_{4,5}$ **as a function of** μ **when** $q_1 = 0.99992, q_2 = 0.99996, A_1 = 0.15, A_2 = 0.2, A_3 = 0.1$ **and** $\varepsilon' = 0.001$

4. ZERO VELOCITY SURFACES

Hills surfaces in the restricted three-body problem give the possibilities to find out some general properties of the relative motion of the third body having infinitesimal mass in the gravitational field of two main bodies with finite masses. The equations of motion (4), admits the Jacobi integral

$$C + \dot{x}^2 + \dot{y}^2 = 2U$$

where C is the Jacobi constant.

Hence, the zero velocity surfaces are:

$$2U - C = 0 \tag{18}$$

The expression (18) and the knowledge of the Lagrangian points allows for us to make a qualitative analysis of the zero velocity surfaces for the binary system **Kruger 60**, under the effects of perturbation in the centrifugal force, radiation pressures, oblateness of the involved bodies and the P-R drag. Plots of the zero velocity surfaces using equation (17) and (18) for different values of the parameters are presented in Fig.s 6-10, and the contour plot in Fig. 11.

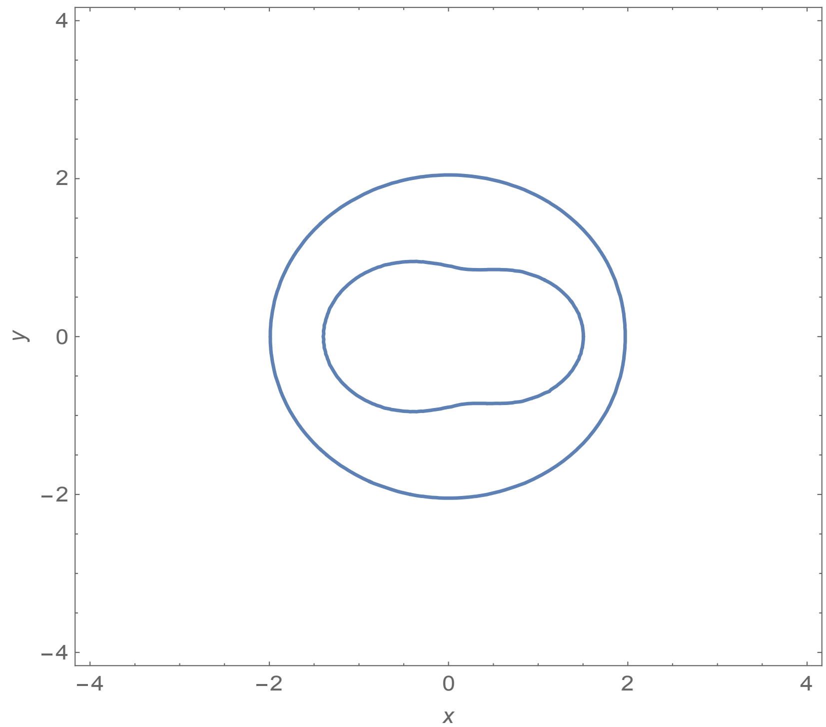

Fig. 6. Zero velocity curve when $q_1 = 0.99992, q_2 = 0.99996, W_1 = 2.6\times10^{-3}$ **and** $W_2 = 1.8\times10^{-4}$

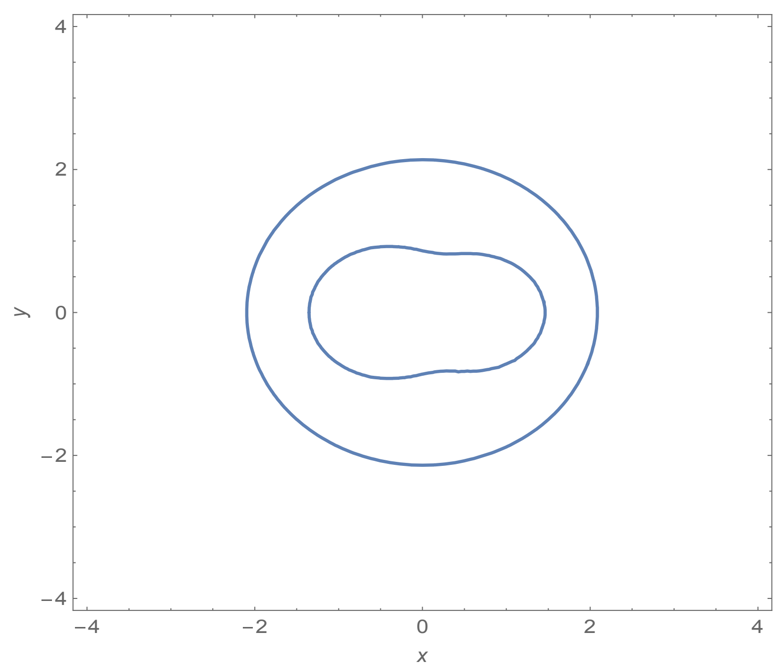

Fig. 7. Zero velocity curve when $q_1 = 0.99992, q_2 = 0.99996, W_1 = 2.6\times10^{-3}, W_2 = 1.8\times10^{-4}$ **and** $A_1 = 0.15$

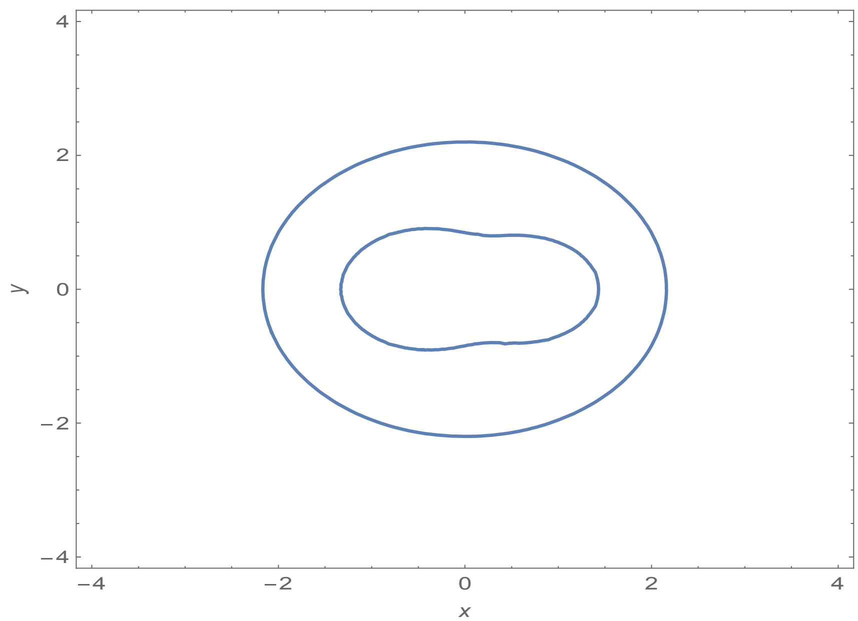

Fig. 8. Zero velocity curve when $q_1 = 0.99992, q_2 = 0.99996, W_1 = 2.6\times10^{-3}, W_2 = 1.8\times10^{-4}, A_1 = 0.15, A_2 = 0.2$ **and** $A_2 = 0.1$

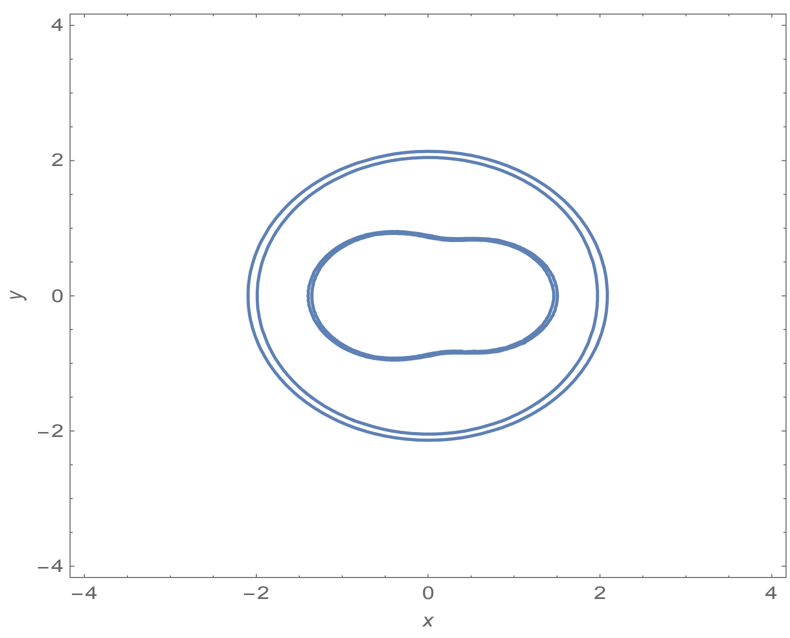

Fig. 9. Variations in the Zero velocity curves when $\mu = 0.3937$ **,** $q_1 = q_2 = 1$**,** $W_1 = W_2 = 0$**,** $A_1 = A_2 = A_3 = 0$ **and when** $\mu = 0.3937$ **,** $q_1 = 0.99992$ **,** $q_2 = 0.99996$ **,** $W_1 = 2.6\times10^{-3}$**,** $W_2 = 1.8\times10^{-4}$**,** $A_1 = 0.15$

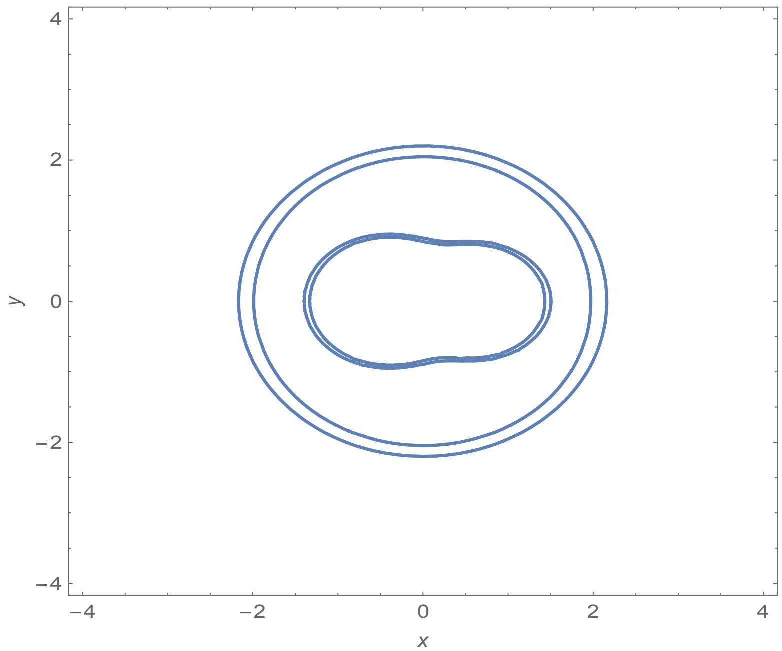

Fig. 10. Variations in the Zero velocity curves when $\mu = 0.3937$ **,** $q_1 = q_2 = 1$**,** $W_1 = W_2 = 0$**,** $A_1 = A_2 = A_3 = 0$ **and when** $\mu = 0.3937$ **,** $q_1 = 0.99992$ **,** $q_2 = 0.99996$ **,** $W_1 = 2.6\times10^{-3}$**,** $W_2 = 1.8\times10^{-4}$**,** $A_1 = 0.15$ **,** $A_2 = 0.2$ **and** $A_3 = 0.1$

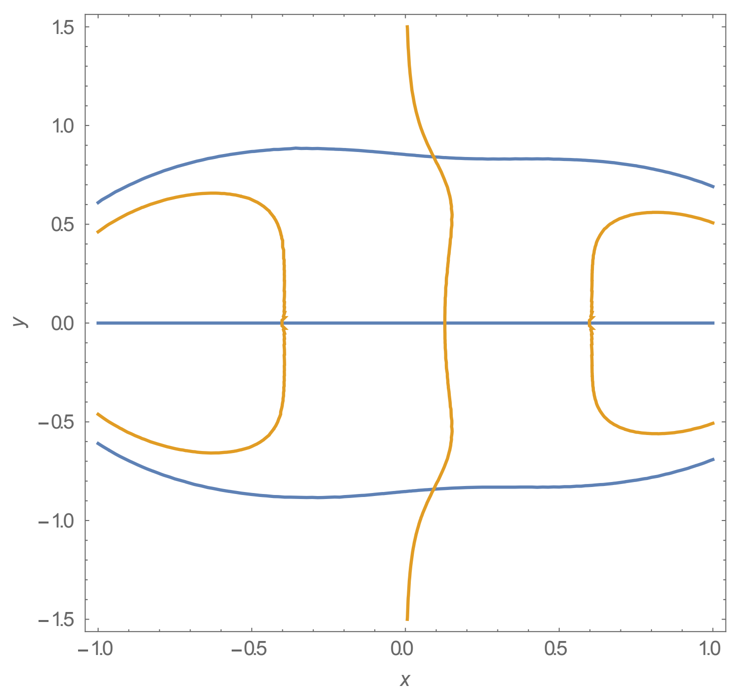

Fig. 11. Contour plot of the region of motion when $q_1 = 0.99992$, $q_2 = 0.99996$, $W_1 = 2.6\times10^{-3}$, $W_2 = 1.8\times10^{-4}$, $A_1 = 0.15$, $A_2 = 0.2$ **and** $A_2 = 0.1$

5. STABILITY OF TRIANGULAR LAGRANGIAN POINTS

In the work of Singh and Haruna [10], the triangular points are linearly stable under effect of perturbations in the Coriolis and centrifugal forces, radiation pressure of the primaries and oblateness of the three bodies. Hence, it is worthwhile to discuss the stability of triangular equilibrium points under additional influence of the P-R drag of the primaries.

Now, to examine the stability of the triangular Lagrangian points, we denote the location by (a_0, b_0) and let (ξ, η) be a small displacement from the location, such that $x = a_0 + \xi$ and $y = b_0 + \eta$. Substituting these values in (4), we obtain the variational equations

$$\begin{aligned} \ddot{\xi} - 2n\alpha\dot{\eta} &= (U_{x\dot{x}})^0 \dot{\xi} + (U_{x\dot{y}})^0 \dot{\eta} + (U_{xx})^0 \xi + (U_{xy})^0 \eta \\ \ddot{\eta} + 2n\alpha\dot{\xi} &= (U_{y\dot{x}})^0 \dot{\xi} + (U_{y\dot{y}})^0 \dot{\eta} + (U_{yx})^0 \xi + (U_{yy})^0 \eta \end{aligned} \tag{19}$$

where, only linear terms in ξ and η have been retained. The second order partial derivatives of U are denoted by subscripts 0and indicates that the derivatives are to evaluated at the Lagrangian point (a_0, b_0).

The corresponding characteristic equation of equations (19) is

$$\begin{aligned} &\lambda^4 - \left(U^0{}_{y\dot{y}} + U^0{}_{x\dot{x}}\right)\lambda^3 + \left[4n^2\alpha^2 + U^0{}_{x\dot{x}}U^0{}_{y\dot{y}} - U^0{}_{xx} - U^0{}_{yy} - (U^0{}_{x\dot{y}})^2\right]\lambda^2 + \left(U^0{}_{x\dot{x}}U^0{}_{yy}\right. \\ &\left. + U^0{}_{xx}U^0{}_{y\dot{y}} + 2nU^0{}_{xy} - 2nU^0{}_{yx} - U^0{}_{y\dot{x}}U^0{}_{xy} - U^0{}_{yx}U^0{}_{x\dot{y}}\right)\lambda + U^0{}_{xx}U^0{}_{yy} - U^0{}_{yx}U^0{}_{xy} = 0. \end{aligned} \tag{20}$$

Where

$$\begin{aligned} U^0_{x\dot{x}} &= -(x_0 + \mu)^2 W_1 - W_1 - (x_0 + \mu - 1)^2 W_2 - W_2 \\ U^0_{x\dot{y}} &= -(x_0 + \mu) y_0 W_1 - (x_0 + \mu - 1) y_0 W_2 = U^0_{y\dot{x}} \\ U^0_{y\dot{y}} &= -\left(y_0^2 + 1\right)W_1 - \left(y_0^2 + 1\right)W_2 \\ U^0_{xx} &= 3x_0^2 - 3\mu^2 + 3\mu + 2\left(x_0^2 + 2\mu x_0 + \mu^2 - \mu^2 x_0 - 2\mu^2 x_0 - \mu^3\right)(1 - q_1) \\ &+ 2\left(\mu x_0^2 + \mu^3 + 2\mu^2 x_0 - 2\mu x_0 - 2\mu^2 + \mu\right)(1 - q_2) + 5\left(x_0^2 - \mu^2 + \mu\right)\varepsilon' \\ &+ \frac{3}{2}\left(\mu + 5x_0^2 + 10\mu x_0 + 5\mu^2 - 5\mu x_0^2 - 10\mu^2 x_0 - 5\mu^3\right)A_1 \\ &+ \frac{3}{2}\left(1 + 4\mu + 5\mu x_0^2 + 5\mu^3 + 10\mu^2 x_0 - 10\mu x_0 - 10\mu^2\right)A_2 - \frac{3}{2}\left(1 - 5x_0^2 + 5\mu^2 - 5\mu\right)A_3 \\ &+ 3\left(1 - \mu - 5\mu^2 + 5\mu^3 + 2x_0 - 5x_0^2 - 10\mu x_0 + 5\mu x_0^2 + 10\mu^2 x_0\right)\varepsilon_1 \\ &- 3\left(4\mu - 10\mu^2 + 5\mu^3 + 2x_0 + 5\mu x_0^2 - 10\mu x_0 + 10\mu^2 x_0\right)\varepsilon_2 \\ &- 2\left(x_0 y_0 + \mu y_0\right)W_1 - 2\left(x_0 y_0 + \mu y_0 - y_0\right)W_2 \end{aligned}$$

$$U_{yx}^{0} = 3x_0 y_0 + 2\left(x_0 y_0 - \mu\, y_0 - \mu\, x_0 y_0 - \mu^2 y_0\right)(1-q_1) + 2\left(\mu x_0 y_0 + \mu^2 y_0 - \mu\, y_0\right)(1-q_2)$$
$$+\frac{15}{2}\left(x_0 y_0 + \mu\, y_0 - \mu x_0 y_0 - \mu^2 y_0\right)A_1 + \frac{15}{2}\left(\mu x_0 y_0 + \mu^2 y_0 - \mu\, y_0\right)A_2 + \frac{15}{2}\left(x_0 y_0\right)A_3 + 5\left(x_0 y_0\right)\varepsilon'$$
$$+\frac{3}{2}\left(2y_0 + \frac{x_0}{y_0} - 10x_0 y_0 - 10\mu\, y_0 + 10\mu x_0 y_0 + 10\mu^2 y_0\right)\varepsilon_1 - \frac{3}{2}\left(2y_0 - \frac{x_0}{y_0} - 10\mu\, y_0 + 10\mu x_0 y_0 + 10\mu^2 y_0\right)\varepsilon_2$$
$$+2\left(x_0 + \mu\right)^2 W_1 - W_1 + 2\left(x_0 + \mu - 1\right)^2 W_2 - W_2$$
$$U_{yy}^{0} = 3y_0^2 + 2\left(y_0^2 - \mu\, y_0^2\right)(1-q_1) + \left(2\mu\, y_0^2\right)(1-q_2) + \frac{3}{2}\left(\mu + 5y_0^2 - 5\mu\, y_0^2\right)A_1 + \frac{3}{2}\left(1-\mu+5\mu\, y_0^2\right)A_2 - \frac{3}{2}\left(1-5y_0^2\right)A_3 + 5y_0^2\varepsilon'$$
$$+3\left(2-\mu-5y_0^2+5\mu\, y_0^2\right)\varepsilon_1 + 3\left(1+\mu-5\mu\, y_0^2\right)\varepsilon_2 + 2\left(x_0 y_0 + \mu\, y_0\right)W_1 + 2\left(x_0 y_0 + \mu\, y_0 - y_0\right)W_2$$

Substituting equations (11), (13) and (16) in the partial derivatives, we get

$$\lambda^4 + a\lambda^3 + b\lambda^2 + c\lambda + d = 0$$

Where

$$a = 3W_1 + 3W_2$$
$$b = 1 + 8\varepsilon - 3\varepsilon' - \frac{3}{2}(1-2\mu)\left(A_1 + A_2\right) - 3A_3 + \frac{W_1}{\sqrt{3}} - \frac{W_2}{\sqrt{3}}$$
$$c = -\frac{3}{4}(4+3\mu)W_1 - \frac{3}{4}(7-3\mu)W_2$$
$$d = \frac{27}{4}\mu(1-\mu)\left[1 + \frac{22}{9}\varepsilon' + \frac{2}{9}(1-q_1) + \frac{2}{9}(1-q_2) + \frac{13}{3}\left(A_1 + A_2\right) + \frac{4}{3}A_3 - \frac{\left(3\mu^2 - 5\mu + 2\right)W_1}{\sqrt{3}\left(1-2\mu+\mu^2\right)} - \frac{\left(3\mu^2 - 4\mu + 1\right)W_2}{\sqrt{3}\mu\left(1-2\mu+\mu^2\right)}\right]$$

We note that the coefficient of Lambda in the characteristic equation is negative and the equation has at least a change in sign. However, in order to ascertain the kinds of roots of (20), we compute the roots $\lambda_i\left(i = 1,2,3,4\right)$ numerically for the binary system **Kruger 60** in Table 6 for different values of the system parameters.

We see from Table 6 that the four roots of the characteristic equation computed for the binary **Kruger 60** are complex roots in the presence and absence of P-R drag, and even for the classical case. In this case the triangular Lagrangian points are unstable. However, we know from the classical R3BP of Szebehely [2] that in the absence of the P-R drag, conditional stability of the triangular points is possible. Therefore, we cannot say that the instability is as a result of the P-R drag. So we explore further.

Now, in the absence of P-R drag of the primaries, the characteristic equation (20) becomes

$$\lambda^4 + b\lambda^2 + d = 0$$

Table 6. Roots of equation (20) for $\mu = 0.3937$, under radiation pressure, oblateness, perturbations and P-R drag.

q_1	q_2	A_1	A_2	A_3	ε	ε'	W_1	W_2	λ_i
1	1	0	0	0	0	0	0	0	$\pm$ 0.620218 $\pm$ 0.94056i
0.99992	1	0	0	0	0	0	0	0	$\pm$ 0.620223 $\pm$ 0.94057i
0.99992	0.99996	0	0	0	0	0	0	0	$\pm$ 0.620225 $\pm$ 940574i
0.99992	0.99996	0.02	0	0	0	0	0	0	$\pm$ 0.64281 $\pm$ 0.95395i
0.99992	0.99996	0.02	0.01	0	0	0	0	0	$\pm$ 0.65350 $\pm$ 0.96035i
0.99992	0.99996	0.02	0.01	0.015	0	0	0	0	$\pm$ 0.66653 $\pm$ 0.95758i
0.99992	0.99996	0.024	0.02	0.015	0.001	0	0	0	$\pm$ 0.66503 $\pm$ 0.95863i
0.99992	0.99996	0.024	0.02	0.015	0.001	0.003	0	0	$\pm$ 0.66834 $\pm$ 0.95858i
0.99992	0.99996	0.024	0.02	0.015	0.001	0.003	$1.04548*10^{-9}$	0	$\pm$ 0.66834 $\pm$ 0.95858i
0.99992	0.99996	0.024	0.02	0.015	0.001	0.003	$1.04548*10^{-9}$	$.39442*10^{-10}$	$\pm$ 0.66834 $\pm$ 0.95858i

Table 7. Roots of (20) for $\mu = 0.03512$ and critical mass parameter in the absence of P-R drag

q_1	q_2	A_1	A_2	A_3	ε	ε'	W_1	W_2	λ_i	μ_C
1	1	0	0	0	0	0	0	0	$\pm$ 0.595124i & $\pm$ 0.803634i	0.0385209
0.99992	1	0	0	0	0	0	0	0	$\pm$ 0.595136i& $\pm$ 0.803625i	0.0385202
0.99992	0.99996	0	0	0	0	0	0	0	$\pm$ 0.595142i & $\pm$ 0.803621i	0.0385198
0.99992	0.99996	0.02	0	0	0	0	0	0	$\pm$ 0.0790839 $\pm$ 0.701647i	0.0328198
0.99992	0.99996	0.02	0.01	0	0	0	0	0	$\pm$ 0.121089 $\pm$ 0.702668i	0.032192
0.99992	0.99996	0.02	0.01	0.015	0	0	0	0	$\pm$ 0.167786 $\pm$ 0.696227i	0.0277778
0.99992	0.99996	0.024	0.02	0.015	0.001	0	0	0	$\pm$ 0.161716 $\pm$ 0.697662i	0.0284199
0.99992	0.99996	0.024	0.02	0.015	0.001	0.003	0	0	$\pm$ 0.170934 $\pm$ 0.696634i	0.0274033
0.99992	0.99996	0.024	0.02	0.015	0.001	0.003	$1.04548*10^{-9}$	0	$\pm$ 0.170934 $\pm$ 0.696634i	-------
0.99992	0.99996	0.024	0.02	0.015	0.001	0.003	$1.04548*10^{-9}$	$3.39442*10^{-10}$	$\pm$ 0.170934 $\pm$ 0.696634i	--------

Table 8. Roots of (20) for $\mu = 0.01$ and critical mass parameter

q_1	q_2	A_1	A_2	A_3	$\in$	$\in'$	W_1	W_2	λ_i	μ_C
1	1	0	0	0	0	0	0	0	$\pm$ 0.701823i& $\pm$ 0.712352i	0.0385209
0.99992	1	0	0	0	0	0	0	0	$\pm$ 0.26835i& $\pm$ 0.963321i	0.0385202
0.99992	0.99996	0	0	0	0	0	0	0	$\pm$ 0.268352i& $\pm$ 0.963321i	0.0385198
0.99992	0.99996	0.02	0	0	0	0	0	0	$\pm$ 0.285822i& $\pm$ 0.942818i	0.0328198
0.99992	0.99996	0.02	0.01	0	0	0	0	0	$\pm$ 0.294784i& $\pm$ 0.932203i	0.032192
0.99992	0.99996	0.02	0.01	0.015	0	0	0	0	$\pm$ 0.306734i& $\pm$ 0.903778i	0.0277778
0.99992	0.99996	0.024	0.02	0.015	0.001	0	0	0	$\pm$ 0.305053i& $\pm$ 0.908759i	0.0284199
0.99992	0.99996	0.024	0.02	0.015	0.001	0.003	0	0	$\pm$ 0.308052i& $\pm$ 0.902776i	0.0274033
0.99992	0.99996	0.024	0.02	0.015	0.001	0.003	$1.04548*10^{-9}$	0	$\pm$ $5.95422*10^{-8}$+0.308051i $-9.84364*10^{-8}$ $\pm$ 0.902776i	----
0.99992	0.99996	0.024	0.02	0.015	0.001	0.003	$1.04548*10^{-9}$	$3.39442*10^{-10}$	$-1.07762*10^{-7}$ $\pm$ 0.902776i $6.62422*10^{-8}$ $\pm$ 0.308051	----

Where

$$b = 1 + 8\varepsilon - 3\varepsilon' - \frac{3}{2}A_1(1-2\mu) + \frac{3}{2}A_2(-1+2\mu) - 3A_3$$

$$d = \frac{27}{4}\mu(1-\mu) + \frac{33}{2}\mu(1-\mu)\varepsilon' + \frac{3}{2}\mu(1-\mu)(1-q_1) + \frac{3}{2}\mu(1-\mu)(1-q_2) + \frac{117}{4}\mu(1-\mu)A_1 + \frac{117}{4}\mu(1-\mu)A_2 + 9\mu(1-\mu)A_3$$

In this case, the critical mass is Singh and Haruna [10]

$$\mu_C = \frac{1}{2} - \frac{1}{2}\sqrt{\frac{23}{27}} - \frac{1}{9}\left(1+\frac{13}{\sqrt{69}}\right)A_1 + \frac{1}{9}\left(1-\frac{13}{\sqrt{69}}\right)A_2 - \frac{22A_3}{9\sqrt{69}} - \frac{2(1-q_1)}{27\sqrt{69}} - \frac{2(1-q_2)}{27\sqrt{69}} - \frac{76\varepsilon'}{27\sqrt{69}} + \frac{16\varepsilon}{3\sqrt{69}} \quad (21)$$

The existence of distinct pure imaginary roots of (20) will depend on the relation between the mass ratio and equation (21). Consequently, when $\mu < \mu_C$ all four roots $\lambda_i(i = 1,2,3,4)$ are purely imaginary numbers and the triangular Lagrangian points are stable, otherwise they are unstable. To illustrate this, we compute the roots and equation (21) numerically under the perturbing forces in Table 7.

It can be seen from Table 7 that, when both, one or none of the primaries emit radiation pressure, the roots are distinct and imaginary. In these cases, $0.03512 = \mu < \mu_C$ and the triangular points are stable, otherwise when $\mu_C < 0.03512 = \mu$, the roots are complex and induces in instability at these points. From this analysis, we still cannot establish that the PR-drag is responsible for the instability. Since indeed instability is taking place in the absence of the P-R drag.

Next, we consider the Earth-Moon system which has a mass ratio of approximately 0.01. Our reason for considering this mass parameter is that it will always be less that the critical masses computed in Table 7 and all four roots 0f (20) are expected to be imaginary and distinct. Hence, in Table 8, we compute these roots for $\mu = 0.01$ alongside the critical masses as shown below

From Table 8, we see that from row 1 to 7, all four roots are imaginary and distinct under the perturbing forces of radiation pressure, oblateness and small perturbations in the Coriolis and centrifugal forces, a result we may attribute to the fact that $0.01 = \mu < \mu_C$ throughout in Table 8. Now, what happens next at this point is convincing enough to make us reach the conclusion regarding effects of the P-R drag. On row 8 where P-R drag of the first primary is included in the computation of the roots by a very or almost negligible value of 1.04548*10^{-9}, we see that the four roots which all along have been imaginary suddenly turned complex roots and induces instability at the triangular equilibrium points. Hence, we can conclude that the P-R drag is a strong perturbing force which changes stability to instability.

6. DISCUSSION AND CONCLUSION

The R3BP is one of the most important and practical problems in dynamical astronomy and is of great historical and educational relevance. In this paper, we have studied motion and stability of an infinitesimal mass around the triangular Lagrangian points when the three bodies in the configuration are oblate spheroids and both primaries are radiation sources under the Poynting-Robertson drag and small perturbations in the Coriolis and centrifugal forces. The study is an extension of the investigation by Singh and Haruna [10] by including the P-R drag of both primaries into the dynamical system.

The equations governing the dynamical set up of our problem have been derived and presented in equations (4) and are defined by the combined effect of oblateness, perturbations, radiation pressure, P-R drag and the mass parameter. These equations are different from those presented in earlier works by Szebehely [2], Subba Rao and Sharma [24], Schuerman [12], Singh and Ishwar [4], Abdul Raheem and Singh [6], Singh and Leke [9], Singh and Abdulkarim [20], Singh and Haruna [10] and Zotos [25], Singh and Amuda [17].

The Lagrangian solutions of the R3BP are widely used in many branches of astronomy and are important as they mark places where particles either can be trapped (L_4 and L_5) or will pass through with a minimum expenditure of energy. Equation (17) gives the location of the triangular points under the combined effects of perturbation, oblateness, radiation and the P-R drag. These points differ from those of Szebehely [2], SubbaRao and Sharma [24], Schuerman [12], Singh and Ishwar [3], AbdulRaheem and Singh [6], Singh and Leke (2014), Singh and Abdulkarim [20] and Singh and Haruna [10]. Using the software *Mathematica,* we conduct a numerical investigation demonstrating how the dynamical quantities: mass ratio, oblateness of the bodies, radiation factors, P-R drag and small perturbation in the centrifugal force influence the positions of the triangular Lagrangian points, zero velocity surfaces and stability. Our results suggest that though the radiation pressure, oblateness and centrifugal perturbation decrease region of stability, they are not the influential forces of instability but the P-R drag. The P-R drag of one or both primary overrides other effect and changes stability to instability. Hence, the introduction of P-R drag into the formulations of Singh and Haruna [10] initiated a twist in rendering the triangular points unstable.

COMPETING INTERESTS

Authors have declared that no competing interests exist.

REFERENCES

1. Lagrange J. OLuvres' (M.J.A. Serret, Ed.). Vol. 6, published by Gautier-Villars, Paris; 1873.
2. Szebehely VG. Theory of orbits. Yale University, New Haven, Connecticut, Academic Press, New-York and London, The Restricted Problem of Three Bodies; 1967.
3. Sharma RK, Subba Rao PV. Stationary solutions and their characteristic exponents in the restricted three-body problem when the more massive primary is an oblate spheroid. Celestial. Mechanics. 1976;13:137.
4. Singh J, Ishwar B. Stability of triangular points in the generalized photogravitational restricted three-body problem. Bulletin of the Astronomical Society of India. 1999;27:415.
5. Khanna M, Bhatnagar KB. Existence and stability of libration points in the restricted three-body problem when the smaller primary is a triaxial rigid body and the bigger one an oblate spheroid. International Journal of Pure and Applied. Mathematics. 1999;30;721.
6. AbdulRaheem A, Singh J. Combined effects of perturbations, radiation, and oblateness on the stability of equilibrium points in the restricted three-body problem. The Astronomical Journal. 2006;131:1880.
7. Singh J, Leke O. Stability of the photogravitational restricted three-body problem with variable masses. Astrophysics and Space Science. 2010;326:305.
8. Singh J, Leke O, Aishetu U. Analysis of the stability of triangular points in the perturbed photogravitational restricted three-body problem with variable masses. Astrophysics and Space Science. 2010;327:299.
9. Singh J, Leke O. Effects of oblateness, perturbations, radiation and varying masses on the stability of equilibrium points in the restricted three-body problem Astrophysics and Space Science. 2013;344:51.
10. Singh J, Haruna S. Equilibrium points and stability under effects of radiation and perturbing forces in the restricted problem of three oblate bodies. Astrophysics and Space Science. 2014;349:107.
11. Singh J, Amuda TO. Effects of poynting-robertson (P-R) drag, Radiation, and Oblateness on motion around the $L_{4,5}$ equilibrium points in the CR3BP. Journal of Dynamical Systems and Geometric Theories. 2017;15:177.
12. Schuerman DW. The restricted three-body problem including radiation pressure. Astrophysical Journal. 1980;238:337.
13. Murray CD. Dynamical effects of drag in the circular restricted three-body problem. Icarus. 1994;122:465.
14. Ragos O, Zafiropoulos FA. A numerical study of the influence of the study of the Poynting-Robertson effect on the equilibrium points of the photogravitational

restricted three-body problem. Astronomy & Astrophysics. 1995;300:568.
15. Kushvah BS. The effect of radiation pressure on the equilibrium point in the generalized photogravitational restricted three-body problem. Astrophysics and Space Science. 2008;315:231.
16. Das MK, et al. On the out of plane equilibrium points in photogravitational restricted three-body problem. Journal of Astronomy and Astrophysics. 2009;30:177.
17. Singh J, Amuda TO. Stability analysis of triangular equilibrium points in the restricted three-body problem under effects o circumbinary disc, radiation and drag forces. Journal Astronomy and Astrophysics. 2019;40:5.
18. Bhatnagar KB, Hallan PP. The effect of perturbations in Coriolis and centrifugal forces on the linear stability of equilibrium points in the restricted problem of three bodies. Celestial Mechanics. 1978;18: 105.
19. Singh J, Leke O. Analytic and numerical treatment of motion of dust grain particle around triangular equilibrium points with post-AGB binary star and disc. Advances in Space Research. 2014;54:1659.
20. Singh J, Abdulkarim A. Instability of triangular libration points in the perturbed photogravitational R3BP with Poynting-Robertson (P-R) drag. Astrophysics and Space Science. 2014;351:473.
21. Luk'yanov LG. Particular solutions in the restricted problem of three bodies with variable masses. Astronomical Journal of Academy of Sciences of USSR. 1989;66:180.
22. Collins H. Interactional expertise as a third kind of knowledge. Phenomenology and the cognitive sciences. 2004;3:125.
23. Wolfram S. The Mathematica Book, 10th Ed. Wolfram Media, Campaigns; 2017.
24. SubbaRao PV, Sharma RK. A note on the stability of the triangular points of equilibrium in the restricted three-body. Astronomy and Astrodynamics. 1975;43:381.
25. Euaggelos E. Zotos. Fractal basins of attraction in the planar circular restricted three-body problem with oblateness and radiation pressure. Astrophysics and Space Science. 2016;361:181.

Peer-review history:
The peer review history for this paper can be accessed here:
http://www.sdiarticle4.com/review-history/62974